*J. Fluid Mech.* (1982), *vol.* 117, *pp.* 473–491
*Printed in Great Britain*



# Effects of internal heat transfer on the structure of self-similar blast waves

By A. F. GHONIEM,
Department of Mechanical Engineering, University of California, Berkeley, California 94720
M. M. KAMEL,
Department of Mechanical Engineering, Cairo University, Cairo, Egypt
S. A. BERGER AND A. K. OPPENHEIM
Department of Mechanical Engineering, University of California, Berkeley, California 94720

(Received 8 April 1980 and in revised form 18 August 1981)

Profiles of gasdynamic parameters in self-similar blast waves, taking into account the influence of conduction and radiation fluxes due to high temperatures attained at the centre, are determined. In the blast-wave equations these fluxes are expressed in terms of the Fourier law for heat conduction and a differential expression for radiative transport in a semi-grey gas model. Various boundary conditions are considered in order to account for different ways in which blast waves are initiated and driven. Similarity requirements are implemented in the solution by compatible functional forms of gas conductivity and absorptivity, as well as the opacity of the shock front. This formulation yields a two-point boundary-value problem, which is then transformed into an initial-value problem in order to facilitate the integration. As a particular example, a detailed solution for the constant-energy case is obtained, covering the whole range of relative heat-transfer effects expressed in terms of radiative to gasdynamic energy fluxes, from the adiabatic flow field, on one extreme, to the isothermal, on the other.

## 1. Introduction

An analysis of blast waves taking into account internal heat transfer was presented first by Sedov (1959). Effects of conduction only were considered and the functional form of thermal conductivity was prescribed by dimensional considerations to satisfy the similarity condition. Using this form, Korobeinikov, Melinkova & Ryazanov (1961) obtained solutions for a constant-energy as well as for an isothermal blast wave.

Marshak (1958) used the radiation-diffusion approximation to solve both cases of constant-density and constant-pressure fields without invoking conditions of self-similarity. The first of these includes the case of a thermal wave, a situation that exists at initial stages of explosion when the gas motion is negligible, while the second shows the effect of radiation on the inner part of the gasdynamic field where pressure is almost constant. A finite-difference solution for the problem of an expanding high-pressure, high-temperature sphere where radiation is significant was obtained by Brode (1969). NiCastro (1970) and Helliwell (1969) treated the problems of radiating walls, either stationary or moving, generating shocks at the head of self-similar flow fields. Bowen &

Feay (1970) used the method of matched asymptotic expansions to solve the problem of strong explosion for small values of the conduction parameter.

The non-self-similar problem of a blast wave associated with diffusive radiation was analysed by Kim *et al.* (1975), using matched expansions, upon the assumption that the radiation effects are significant only in a boundary layer around the centre of explosion. A similar approach was also used by Kamel *et al.* (1977) to find self-similar solutions.

The purpose of this study was to appraise explicitly the effects of internal heat transfer in self-similar blast waves, with particular attention given to the various modes in which the radiative energy-transport processes can occur. The medium was assumed to be an inviscid, perfect gas, so that the sole effect under study was that of conduction and radiation fluxes driven by the high temperatures prevailing at the centre. The solution to the problem formulated in this manner presents thus a contribution to our systematic parametric investigation of the fundamental properties of blast waves (Oppenheim *et al.* 1971, 1972).

The conduction flux is taken to be proportional to the temperature gradient while the radiation flux is related to both the temperature and its gradient through the differential approximation of an appropriate transport equation. This approximation approaches asymptotically on one side the emission radiation limit and on the other the diffusion radiation limit as the optical thickness of the gas changes from zero to infinity. A semi-gray gas model is also adopted for the optical properties of the medium, where two frequency-averaged coefficients of absorption are used, tending toward the Planck and Rosseland coefficients of absorption in the optically thin and thick radiation limits, respectively. The gas is assumed to be at a local-thermodynamic-equilibrium state dominated by collisions.

In order to comply with similarity conditions, the coefficients of absorption and the conductivity of the gas have to vary in a compatible way with temperature and density. This variation is found to be related to the rate at which the bounding front of the field decays, which, in turn, depends on how energy is deposited in the medium. In addition, the opacity of the front itself is determined by the variation of the total energy of the flow field. Thus, different cases of energy deposition are considered and the parameters of the problem are adjusted accordingly.

When conduction is taken into account the resulting two-point boundary-value problem, consisting of six first-order ordinary differential equations, is reduced to a more tractable initial-value problem by a transformation of variables and an adjustment of the boundary conditions. In the case of purely radiative energy transfer, devoid of any effects of conduction, this method is not applicable and the solutions are obtained by a numerical, iterative, implicit shooting technique. At the same time, various modes of energy deposition are considered, such as constant-energy waves, energy irradiated upon the front, or energy radiated from an inner surface.

Results are obtained for the constant-energy waves over a complete range of heat-transfer effects, from the adiabatic to the isothermal limit, according to the specific nature of the dominant mechanism of heat transfer and its relative magnitude.

## 2. Formulation

Blast waves considered as one-dimensional unsteady flow fields are governed by the following conservation equations:

$$\left.\begin{aligned} \frac{\partial}{\partial t}(\rho r^j) + \frac{\partial}{\partial r}(\rho r^j u) &= 0, \\ \frac{\partial}{\partial t}(\rho r^j u) + \frac{\partial}{\partial r}\left(\rho r^j u\left(\frac{p}{\rho u} + u\right)\right) &= 0, \\ \frac{\partial}{\partial t}(\rho r^j(e+\tfrac{1}{2}u^2)) + \frac{\partial}{\partial r}\left(\rho r^j u\left(e + \frac{p}{\rho} + \tfrac{1}{2}u^2\right)\right) &= -\frac{\partial}{\partial r}(r^j q), \end{aligned}\right\} \tag{1}$$

where $\rho$ is density, $p$ is pressure, $u$ is flow velocity, $e$ is internal energy, and $q$ is the energy flux; the latter can be decomposed into $q_c + q_r$, where $q_c$ = conduction heat flux and $q_r$ = radiative heat flux. $r$ and $t$ are respectively the space and time co-ordinates, and

$$j = \left\{\begin{matrix} 0 & \text{for plane symmetry,} \\ 1 & \text{for line symmetry,} \\ 2 & \text{for point symmetry.} \end{matrix}\right\} \tag{1a}$$

According to Fourier's law of heat conduction

$$q_c = -k\frac{\partial T}{\partial r}, \tag{2}$$

where $k$ is the gas thermal conductivity and $T$ is absolute temperature. Assuming a semi-grey gas (Traugott 1966; Finkleman & Chien 1968) the differential approximation of the radiation-transport equation can be written in the following form for general one-dimensional flow:

$$\frac{\partial}{\partial r}\left(\frac{1}{\alpha_P r^j}\frac{\partial}{\partial r}(r^j q_r)\right) = 3\alpha_R q_r + 4\sigma_S\frac{\partial T^4}{\partial r}, \tag{3}$$

where $\sigma_S$ is the Stefan–Boltzmann constant. In the above

$$\alpha_P \equiv \frac{1}{B}\int_0^\infty \alpha_\nu B_\nu d\nu, \tag{3a}$$

is the Planck frequency-averaged absorptivity, where $\nu$ is frequency, $\alpha_\nu$ is the absorptivity at frequency $\nu$, $B_\nu$ is the frequency-dependent radiation flux described by Planck's function, and

$$B = \int_0^\infty B_\nu d\nu$$

is the total radiation flux of a black body. The other coefficient of absorption that appears in (3) is

$$\alpha_R \equiv \frac{1}{i}\int_0^\infty \alpha_\nu i_\nu d\nu, \tag{3b}$$

where $i_\nu$ is the radiation intensity at frequency $\nu$ and

$$i = \int_0^\infty i_\nu d\nu.$$

At high radiation intensity with small gradients $\alpha_R$ approaches the well-known Rosseland coefficient (cf. Finkleman & Chien 1968).

The above system of equations is supplemented with an equation of state and three constitutive relations for the transport properties. We assume a perfect-gas behaviour of the medium, so that

$$p = \rho RT, \quad e = \frac{1}{\gamma - 1}\frac{p}{\rho} \tag{4}$$

($\gamma$ is the specific heat ratio and $R$ is the gas constant) and power-law variation for $k$, $\alpha_P$ and $\alpha_R$, according to which

$$k = k_0\left(\frac{T}{T_0}\right)^{\beta_c}\left(\frac{\rho}{\rho_0}\right)^{\delta_c}, \quad \alpha_P = \alpha_{P0}\left(\frac{T}{T_0}\right)^{\beta_P}\left(\frac{\rho}{\rho_0}\right)^{\delta_P}, \quad \alpha_R = \alpha_{R0}\left(\frac{T}{T_0}\right)^{\beta_R}\left(\frac{\rho}{\rho_0}\right)^{\delta_R}, \tag{5}$$

where the subscript 0 denotes a reference state. In the above, the exponents are to be determined from gas-property data within the appropriate temperature range; if a self-similar solution is sought, they must also satisfy the similarity requirements.

The physical nature of the flow field imposes boundary conditions, and moreover it provides also two integral relations expressing the principles of global conservation of mass and energy inside the field.

At the blast-wave front one has the usual equations for conservation of mass, momentum, and energy:

$$\left.\begin{aligned} &\rho_a W = \rho_n(W - u_n), \quad p_a + \rho_a W^2 = p_n + \rho_n(W - u_n)^2, \\ &e_a + \frac{p_a}{\rho_a} + \tfrac{1}{2}W^2 + \frac{\bar{q}_n}{\rho_a W} = e_n + \frac{p_n}{\rho_n} + \tfrac{1}{2}(W - u_n)^2, \end{aligned}\right\} \tag{6}$$

where subscript n denotes the state immediately behind the front, a denotes atmospheric conditions and $W$ is the speed of the front itself. Also

$$\bar{q}_n = q_n + q_a, \tag{7a}$$

where $q_n$ is the heat flux transferred from the field to the front while $q_a$ specifies the net energy transported across the front. This latter quantity can be written as

$$q_a = q_0 - q_s, \tag{7b}$$

where $q_0$ is the radiation flux received by the front from external sources and $q_s$ is the flux transmitted through the front to the surroundings. This latter is established according to the opacity of the front and depends on its relative velocity with respect to that of the thermal wave that usually accompanies high-temperature fields (Zel'dovich & Raizer 1967).

The inner boundary of the flow field can be either the centre, i.e. $r = 0$, for which

$$u = 0, \quad q_c = q_r = 0 \tag{8a,b}$$

or it can be an inner surface $r = r_1$ moving at a prescribed velocity $u_1$.

Principles of global conservation of mass and energy are expressed in terms of the following integral relations:

$$\int_0^{r_n} \rho r^j \, dr = \int_0^{r_n} \rho_a r^j \, dr, \tag{9}$$

$$\int_0^{r_n} (e + \tfrac{1}{2}u^2) \rho r^j \, dr = E + \int_0^{r_n} \rho_a e_a r^j \, dr + \int_0^t q_a r_n^j \, dt + \int_0^t q_1 r_1^j \, dt, \tag{10}$$

where $E$ is the blast initiation energy of the field; $q_1$ is the energy deposited on the inner boundary $r_1$ of the field.

## 3. Similarity transformation

The system of differential equations (1) and (3) is first expressed in non-dimensional form. This is accompanied by the introduction of

$$x \equiv \frac{r}{r_n}, \quad \text{and} \quad \xi \equiv \frac{r_n}{r_0} \quad \text{or} \quad y \equiv \frac{1}{M^2}, \quad \text{where} \quad M = M(\xi), \tag{11}$$

as independent variables. Here $M$ denotes the normalized front velocity $W/W_0$, and $r_0$ a reference radius. Associated with that is the front trajectory expressed in terms of its decay parameter

$$\lambda \equiv -2\frac{d\ln W}{d\ln r_n} = -2\frac{d\ln M}{d\ln \xi}. \tag{12}$$

It represents an eigenvalue of the equations. Its value is obtained in the process of satisfying the energy integral (10).

The corresponding dependent variables (cf. Oppenheim *et al.* 1971) are

$$h \equiv \rho/\rho_a, \quad g \equiv p/\rho_a W^2, \quad f \equiv u/W, \quad Q \equiv q/\rho_a W^3. \tag{13}$$

The transformed system admits a self-similar solution if $\partial/\partial\xi = \lambda y \, \partial/\partial y = 0$, i.e. if none of the dependent variables depend on $\xi$, a condition satisfied either by letting $\lambda = 0$ or $y = 0$. The latter is the strong-shock limit or the cold-atmosphere approximation associated with $M = \infty$. At the same time, since $\lambda = \lambda(\xi)$, for self-similarity $\lambda$ must be constant. Upon integration, (12) yields the velocity and the trajectory of the front in terms of $M$, $\xi$, and $\tau \equiv t/t_0$, the non-dimensional time, as follows:

$$M = \xi^{-\frac{1}{2}\lambda}, \quad \xi = \tau^{\lambda/(\lambda-2)}, \tag{14}$$

whence

$$W_0 = \frac{r_0}{\frac{1}{2}(\lambda-2)t_0}.$$

Noting that for self-similar flow all the variables are functions of $x$ only while $e_a = 0$, the energy integral (10) can be expressed as follows:

$$W^2 r_n^{j+1} J = \frac{E}{\rho_a} + Q_a \int_0^t W^3 r_n^j \, dt + Q_1 \int_0^t W^3 r_1^j \, dt,$$

where

$$J \equiv \int_0^1 (\sigma + \tfrac{1}{2}f^2) h x^j \, dx, \quad \sigma \equiv \frac{e}{W^2}.$$

Hence, using (14) one gets

$$\xi^{j+1-\lambda}\left(J-\frac{Q_a+x_1^j Q_1}{j+1-\lambda}\right)=\Sigma, \tag{15}$$

where

$$\Sigma \equiv \frac{E}{\rho_a W_0^2 r_0^{j+1}}$$

is the specific blast initiation energy.

The similarity restrictions on both the value of $\lambda$ and the front opacity can be found by requiring (15) to be either independent of $\xi$ or by setting its right-hand side equal to zero. Two cases are thus realized.

(*a*) If $\Sigma \neq 0$ then

$$\lambda = j+1, \quad Q_a + x_1^j Q_1 = 0. \tag{16a,b}$$

The above implies that, if a blast wave is generated by an instantaneous deposition of energy, its bounding front must be opaque or its net exchange of energy with the surroundings must be zero in order to satisfy the energy-conservation requirement for self-similarity.

(*b*) If $\Sigma = 0$, one has

$$\lambda = j+1-\frac{Q_a+x_1^j Q_1}{J}. \tag{17a}$$

This is the case of a blast wave driven by radiation supplied on either its front or on an inner boundary. It should be noted that in order to satisfy the similarity requirements the inner boundary should move according to a law similar to the front trajectory given by (14). The case of a stationary radiating wall can be recovered only for the plane case, for which $j = 0$ and

$$\lambda = 1-\frac{Q_a+Q_1}{J}. \tag{17b}$$

In (5) the values of $\beta_c$, $\beta_P$ and $\beta_R$ that satisfy the similarity condition can be obtained by requiring that $Q_c$ and $Q_r$ based respectively on (2) and (3) be independent of the front Mach number $M$. Thus, substituting (5) into (2) and (3), and using the definitions (13) of the non-dimensional variables along with the equations of state (4), one obtains

$$Q_c = -\frac{k_0 T_0}{\rho_0 r_0 W_0^3} M^{-1-2\beta_c+2/\lambda} \theta^{\beta_c} h^{\delta_c} \frac{\partial \theta}{\partial x}, \tag{18}$$

$$\frac{\rho_0 W_0^3}{\alpha_{P0} r_0 \sigma_S T_0^4} \frac{M^{-5-2\beta_P+2/\lambda}}{x^j} \frac{\partial}{\partial x}\left(h^{-\delta_P}\theta^{-\beta_P} x^j \frac{\partial Q_r}{\partial x}\right)$$

$$= 3\frac{\rho_0 W_0^3 \alpha_{R0} r_0}{\sigma_S T_0^4} M^{-5+2\beta_R-2/\lambda} h^{\delta_R} \theta^{\beta_R} Q_r + 4\frac{\partial \theta^4}{\partial x}, \tag{19}$$

where $\theta \equiv \gamma g/h$, the non-dimensional temperature. It should be noted here that the reference density $\rho_0$ is taken to be the same as the density $\rho_a$ of the surrounding atmosphere.

Setting the exponents of $M$ equal to zero yields the following values for $\beta$:

$$\beta_c = \frac{1}{2} - \frac{1}{\lambda}, \tag{20}$$

$$\beta_P = \frac{1}{\lambda} - \frac{5}{2}, \quad \beta_R = \frac{1}{\lambda} + \frac{5}{2}. \tag{21}$$

Similar expressions for the $\beta$'s were obtained earlier by Sedov (1959), Elliot (1960), Helliwell (1969) and NiCastro (1970) by the use of dimensional analysis. The expressions given above show the effect of the process of energy exchange as well as that of geometry, reflected by the dependence of the $\beta$ on the decay parameter $\lambda$.

With the exponents of $M$ equal to zero, (18) and (19) reduce to

$$Q_c = -\Gamma_c \theta^{\beta_c} h^{\delta_c} \frac{d\theta}{dx}, \tag{22}$$

$$\frac{1}{\Gamma_P} \frac{d}{dx}\left(\frac{\theta^{-\beta_P} h^{-\delta_P}}{x^j} \frac{d}{dx}(x^j Q_r)\right) = \frac{3}{\Gamma_R} h^{\beta_R} \theta^{\delta_R} Q_r + 4\frac{d\theta^4}{dx}, \tag{23}$$

where

$$\Gamma_c \equiv \frac{k_0 T_0}{\rho_0 r_0 W_0^3}, \quad \Gamma_P \equiv \frac{\kappa}{B_z}, \quad \Gamma_R \equiv \frac{1}{\kappa B_z}, \tag{24a,b,c}$$

while

$$\kappa \equiv r_0 \alpha_0 = r_0/l_0, \quad B_z \equiv \frac{\rho_0 W_0^3}{\sigma_S T_0^4}. \tag{25a,b}$$

In the above, $B_z$ is the Boltzmann number, which shows the relative contribution of radiation in energy-transfer processes; the Bouguer number $\kappa$ is the characteristic optical thickness of the gas, which indicates the dominant mechanism of radiative energy transfer; $l_0$ is the radiation mean free path. Similar dimensionless parameters were used by Goulard (1962) and Vincenti & Kruger (1975) to describe radiation effects in gasdynamics.

The parameters $\Gamma_c$, $\Gamma_P$ and $\Gamma_R$ defined by (24) express the relative effects of conduction, radiative emission and radiative diffusion, respectively, in comparison to energy transfer by convective processes. The value of $\kappa$, the optical thickness of the gas, determines the dominant mechanism of radiative energy transfer.

The boundary conditions at the front, after transformation into non-dimensional variables and setting $y = 0$, as required by similarity, take the form

$$h_n = \frac{1}{1-f_n}, \quad g_n = f_n, \quad \bar{Q}_n = \frac{\gamma+1}{2(\gamma-1)} f_n \left(\frac{2}{\gamma+1} - f_n\right). \tag{26a,b,c}$$

## 4. The boundary-value problem

The transformed equations of motion, based on the general form presented by Oppenheim *et al.* (1971), can be now recast as follows:

$$\frac{dh}{dx} = \frac{h}{x(1-F)}\left\{(j+1)F + x\frac{dF}{dx}\right\}, \tag{27a}$$

$$\frac{dF}{dx} = \frac{(j+1)F\frac{\theta}{x^2} + \frac{(1-F)}{x}\frac{d\theta}{dx} - \gamma F(1-F)(\frac{1}{2}(\lambda+2) - F)}{x\{\gamma(1-F)^2 - \theta/x^2\}}, \tag{27b}$$

$$\frac{d\theta}{dx} = -\theta^{-\beta_c} h^{-\delta_c} \Gamma_c^{-1} Q_c, \tag{27c}$$

$$\frac{dQ}{dx} = -j\frac{Q}{x} - \frac{h\theta}{\gamma(\gamma-1)}\left\{-\lambda - (1-F)\frac{x}{\theta}\frac{d\theta}{dx} + (\gamma-1)(1-F)\frac{x}{h}\frac{dh}{dx}\right\}, \tag{27d}$$

$$\frac{dI}{dx} = \frac{3}{\Gamma_R} h^{\delta_R} \theta^{\beta_R} Q_r + 16\theta^3 \frac{d\theta}{dx}, \tag{27e}$$

$$\frac{dQ_r}{dx} = -j\frac{Q_r}{x} + \Gamma_p \theta^{\beta_p} h^{\delta_p} I, \tag{27f}$$

where $F \equiv f/x$, $Q = Q_r + Q_c$, $I \equiv i/\rho_a W^3$, while

$$i \equiv \frac{1}{\alpha_p r^j}\frac{\partial}{\partial r}(r^j q_r).$$

In the constant-energy case, where $\lambda = j+1$, (27*d*) can be integrated analytically to a closed expression for the energy flux:

$$Q = hx^3\left\{\left(\frac{\theta}{\gamma(\gamma-1)x^2} + \tfrac{1}{2}F^2\right)(1-F) - \frac{\theta F}{\gamma x^2}\right\}. \tag{28}$$

This set of equations is subject to the following boundary conditions.

(i) At $x = 1$, (26) specify the boundary conditions at the front; in particular, noting that $F_n = f_n$, (26*a*, *b*) yield

$$\theta_n \equiv \frac{\gamma g_n}{h_n} = \gamma F_n(1-F_n). \tag{29}$$

(ii) At $x = 0$, (8*a*) imposes the condition $f_1 = 0$, while from (8*b*) it follows that $Q_r = 0$ and $d\theta/dx = 0$. Since $F = f/x$, then, at $x = 0$, $F = df/dx$. From the continuity equation, since $dh/dx = 0$, one has $df/dx = 0$, thus

$$F_1 = 0. \tag{30}$$

The above formulation constitutes a two-point boundary-value problem in six first-order ordinary differential equations (27). The solution can be reduced significantly if the problem is transformed into an initial-value problem as described in § 5.

## 5. Transformation into initial-value problem

If the equations are to be integrated numerically starting from $x = 0$, the values of $h_1$ and $\theta_1$ must be known; however, one of the purposes of integrating these equations is to obtain these values. It was observed earlier by Elliot (1960), in a similar problem, that the equations will retain the forms given by (27) when the following normalized variables are introduced

$$\tilde{\theta} \equiv \theta/\theta_1, \quad \tilde{h} \equiv h/h_1, \quad \tilde{I} \equiv I/I_1, \quad \tilde{x} \equiv x/x^*, \quad \tilde{Q} \equiv Q/Q^*, \tag{31}$$

if $x^*$, $Q^*$, $I_1$ are

$$x^* = \theta_1^{\frac{1}{2}}, \quad Q^* = h_1 x^{*3}, \quad I_1 = \theta_1^4, \tag{32}$$

and the $\Gamma$ are expressed as

$$\left.\begin{aligned}\Gamma_{\mathrm{c}}^{*} &= h_1^{(\delta_{\mathrm{c}}-1)}\,\theta_1^{(\beta_{\mathrm{c}}-1)}\,\Gamma_{\mathrm{c}},\\ \Gamma_{\mathrm{P}}^{*} &= h_1^{(\delta_{\mathrm{P}}-1)}\,\theta_1^{(\beta_{\mathrm{P}}+3)}\Gamma_{\mathrm{P}},\\ \Gamma_{\mathrm{R}}^{*} &= h_1^{-(1+\delta_{\mathrm{R}})}\,\theta_1^{(2-\beta_{\mathrm{R}})}\Gamma_{\mathrm{R}}.\end{aligned}\right\} \tag{33}$$

Initial conditions at $\tilde{x} = x = 0$ are

$$F_1 = 0, \quad \tilde{\theta}_1 = \tilde{h}_1 = 1. \tag{34a,b}$$

For an adiabatic inner boundary, $\tilde{Q}_{\mathrm{r}} = \tilde{Q}_{\mathrm{c}} = 0$ and $\tilde{I}_1 = 1$.

As a consequence of the above,

$$\frac{dF}{dx} = \frac{dh}{dx} = \frac{d\theta}{dx} = 0; \tag{34c}$$

while

$$\frac{dQ}{dx} = \frac{\lambda}{\gamma(\gamma-1)(j+1)}, \quad \frac{dI}{dx} = 0, \tag{34d}$$

$$\frac{dQ_{\mathrm{r}}}{dx} = \frac{4\Gamma_{\mathrm{P}}}{j+1}. \tag{34e}$$

The outer boundary is reached when the relation

$$\tilde{\theta}_{\mathrm{n}} = \gamma\tilde{x}_{\mathrm{n}}^2 F_{\mathrm{n}}(1-F_{\mathrm{n}}) \tag{35a}$$

is satisfied. At this point $x_1$ and $h_1$ can be evaluated, since, according to (26*a*),

$$h_{\mathrm{n}} = \frac{1}{1-F_{\mathrm{n}}}. \tag{35b}$$

Equation (26*c*) can be used to determine $\bar{Q}_{\mathrm{n}}$ while the value of $Q_{\mathrm{n}}$ is evaluated during the course of calculation. Equation (17) is then used to check the accuracy of the solution.

## 6. Limiting cases

When $\kappa$ approaches 0 or $\infty$ the radiative-transfer equation (23) leads to two limiting cases.

The first limit, referred to as the Planck emission approximation, corresponds to $\kappa = 0$, the optically thin gas. In this case $\Gamma_{\mathrm{R}} \to \infty$, and by integrating (23) one obtains

$$\frac{d}{dx}(x^j Q_{\mathrm{r}}) = 4\Gamma_{\mathrm{P}} x^j h^{\delta_{\mathrm{P}}}\theta^{4+\beta_{\mathrm{P}}}, \tag{36}$$

which can be used to replace (27*e,f*).

The second limit, referred to as the Rosseland diffusion approximation, corresponds to $\kappa = \infty$, the optically thick gas. In this case $\Gamma_{\mathrm{P}} \to \infty$, the left-hand side of (23) is equal to zero, yielding an explicit expression for the radiation flux:

$$Q_{\mathrm{r}} = -\tfrac{16}{3}\Gamma_{\mathrm{R}} h^{-\delta_{\mathrm{R}}}\theta^{3-\beta_{\mathrm{R}}}\frac{d\theta}{dx}. \tag{37}$$

The characteristic features of physical situations where these limits apply can be deduced from the definition of $\kappa$. In the case of a constant-energy wave an expression for $r_0$ can be obtained in the form $(E/\rho_0 W_0^2)^{1/(j+1)}$. Thus, for low-density conditions and relatively small blast energies, $r_0$ is small and $l_0$ is large (cf. Thomas & Penner 1964); the value of $\kappa$ is, according to (25*a*), small, and the gas is radiatively 'thin'. This is typical of laboratory conditions. On the other hand, for normal densities and large explosion energies, the characteristic dimension $r_0$ is large, the radiation mean free path $l_0$ is small and $\kappa$ is consequently large. This is the case of radiative diffusion typical of large-scale explosions.

## 7. Singular case

When conduction is neglected, $\Gamma_c = 0$, and (27*c*) cannot be used to evaluate the temperature gradient. Also, since in this case $Q = Q_r$ (27*d*) and (27*f*) specify the same quantity and become equivalent. To overcome these difficulties, a modified formulation is required. First, (23) is rearranged and split in the following way:

$$\frac{dI}{dx} = -3\frac{\theta^{\beta_R} h^{\delta_R}}{\Gamma_R} Q_r, \tag{38}$$

$$\frac{1}{x^j}\frac{d}{dx}(x^j Q_r) = \Gamma_P \theta^{\beta_P} h^{\delta_P}(4\theta^4 - I), \tag{39}$$

where the quantity $I$ defined above is different from $I$ defined in (27*e*), and is the radiation intensity averaged with respect to both frequency and solid angle. Solving (27*d*) in terms of the temperature gradient and then using (39) to eliminate the flux gradient, we obtain

$$\frac{d\theta}{dx} = -\frac{(\gamma-1)\theta}{h}\frac{dh}{dx} - \Psi_1, \tag{40}$$

where

$$\Psi_1 = \frac{\theta}{x(1-F)}\{\lambda - \gamma(\gamma-1)\Gamma_P \theta^{(\beta_P-1)} h^{(\delta_P-1)}(4\theta^4 - I)\}.$$

Finally, (27*a*, *b*) and (40) are solved algebraically to find the derivatives of the gas-dynamic variables as

$$\frac{dh}{dx} = \frac{\Psi_4 \Psi_2}{\Psi_2 - (\gamma-1)\theta}, \tag{41}$$

$$\frac{dF}{dx} = \frac{(1-F)}{h}\left(\frac{dh}{dx} - \Psi_2\right), \tag{42}$$

$$\frac{d\theta}{dx} = \frac{(\gamma-1)\theta}{h}\frac{dh}{dx} - \Psi_1, \tag{43}$$

where

$$\Psi_2 = \gamma x^2(1-F)^2 - \theta,$$

$$\Psi_3 = (j+1)F\theta - \gamma x^2 F(1-F)\left(\frac{\lambda+2}{2} - F\right),$$

$$\Psi_4 = \frac{(j+1)Fh}{x(1-F)} + \frac{h}{\Psi_2}\left(\frac{\Psi_3}{x(1-F)} - \Psi_1\right).$$

The change in the boundary conditions is even more profound in this case since $d\theta/dx \neq 0$ and consequently $F \neq 0$ at the centre, $x = 0$. On the other hand, while $Q = 0$ must still be satisfied, this condition does not yield an explicit expression for the derivatives there. It should be noted that (41)–(43) do not include $Q$ but only its derivative. (Even though $Q = 0$ at the centre is not imposed, all of the numerical solutions calculated are found to have this property.) Thus we are left with only the boundary conditions $f = 0$ at $x = 0$ and (26) at $x = 1$.

## 8. Results

An explicit fourth-order Runge–Kutta integration scheme, with variable step to achieve the desired accuracy, was used to compute the solution of (27), with conduction taken into account, for the two radiation limits, Planck and Rosseland. In the former limit (27*e*) is replaced by (36), and in the latter (27*f*) is replaced by (37). In both cases the integration starts from the centre, $x = 0$, a saddle-point singularity, where all the gasdynamic variables and their derivatives, defining the centre line of the saddle, are given. When (34*a*) is satisfied, the front is located and the normalizing parameters are evaluated from (32). The first set of results presented are for the cases of Planck radiative emission and Rosseland radiative diffusion, both associated with conduction, where $\Gamma_c$ is always kept at 0·001, while $\Gamma_P$ and $\Gamma_R$ change from 0 to $\infty$, covering a full spectrum of cases from adiabatic to isothermal. Solutions have been obtained for a point explosion, i.e. for a constant-energy field with spherical symmetry.

The medium was considered to behave as a perfect gas with the specific heat ratio $\gamma = 1{\cdot}4$, while the dependence of gas conductivity and absorptivity on density was expressed in terms of the following exponents (cf. (5)): $\delta_c = 1$, $\delta_P = \delta_R = 2$. This is representative of the case of high-temperature, low-density air (Thomas & Penner 1964).

Figures 1(*a*), (*b*) present solutions in the phase plane for the case of Planck radiative emission and Rosseland radiative diffusion, respectively, where $Z \equiv \theta/x^2$. The $P_{G\infty}$ line is the Hugoniot curve for a radiation-driven shock wave, given by

$$Z = \gamma(1-F)F.$$

As the energy deposited by radiation on the shock front increases owing to higher values of $\Gamma$, the shock location shifts along this curve to the left. The displacement of the front on the $P_{G\infty}$ curve as $\Gamma$ increases is a result of the fact that higher radiation fluxes are transmitted to an opaque front. (The opacity of the front was determined from the similarity requirement that exists in the initial stages of propagation.) This situation resembles the case of a blast wave headed by a detonation front where energy is deposited due to chemical reaction. The isothermal field is represented by the dashed line. All the integral curves lie to the right of the curve

$$D \equiv Z-(1-F)^2 = 0,$$

except for the isothermal field curve which crosses it at a saddle-point singularity (Korobeinikov *et al.* 1961).

Although the two sets of curves depict the same trend, a shift to the left with increasing $\Gamma$, it should be noticed that the curves corresponding to the Rosseland radiative diffusion approach the isothermal limit faster and at smaller values of $\Gamma$ than

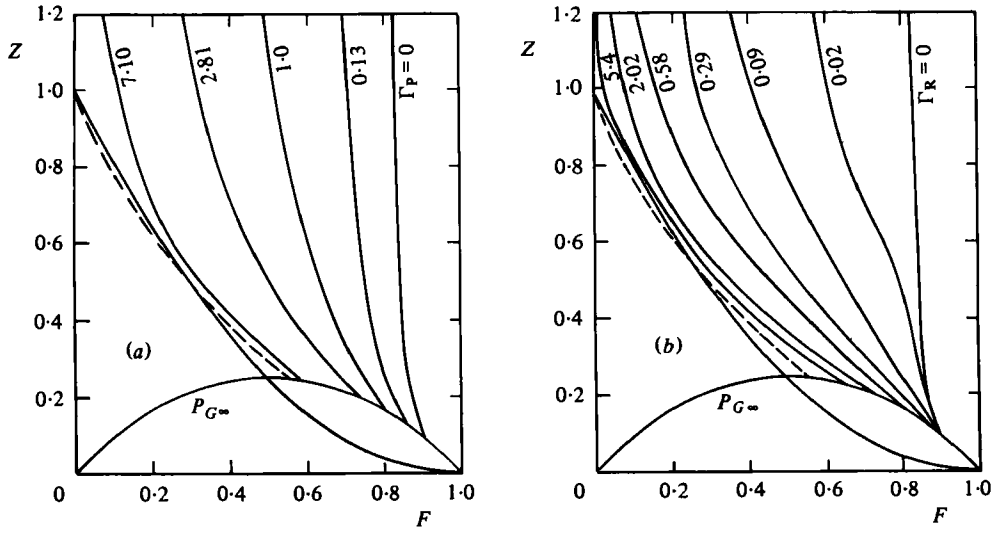


FIGURE 1. Phase planes for a point explosion for the cases of (*a*) Planck radiative emission and (*b*) Rosseland radiative diffusion. In both cases, conduction is taken into account with $\Gamma_c = 0{\cdot}001$ while $\Gamma_P$ and $\Gamma_R$ take on values from 0 to $\infty$. The broken line is the integral curve for the isothermal blast wave. The front moves along the line $P_{G\infty}$. All curves with finite values of $\Gamma$ approach asymptotically $F = 0$ at $Z = \infty$.

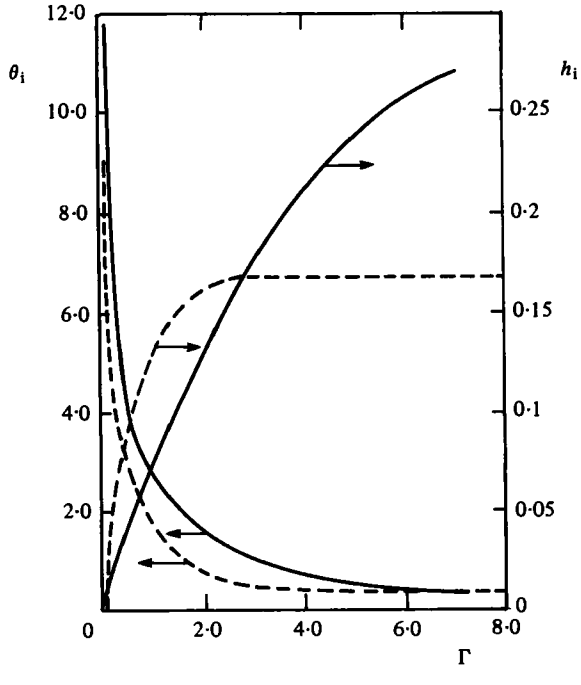


FIGURE 2. Variation of density and temperature with $\Gamma$ at the centre of explosion. Planck radiative emission is shown as solid lines, Rosseland radiative diffusion as broken lines. $\Gamma_c = 0{\cdot}001$ for both cases.

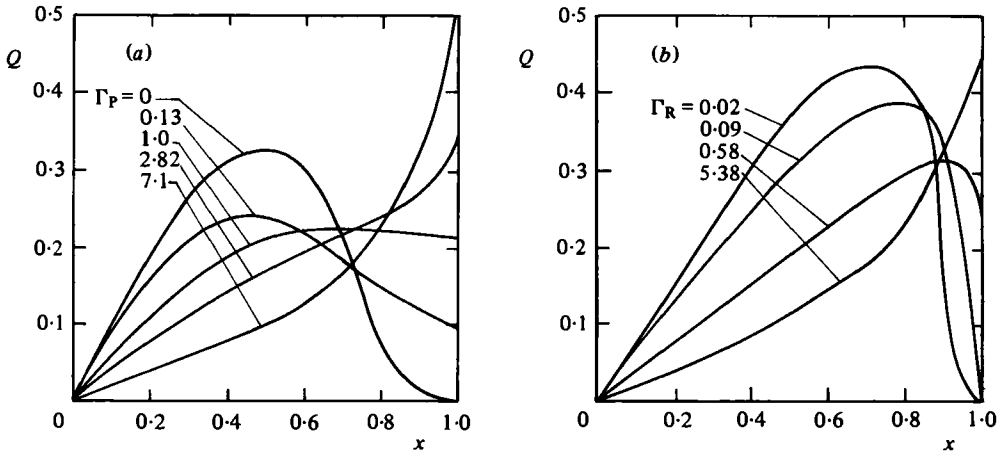


FIGURE 3. Total heat flux of conduction and radiation for different values of the radiation parameter $\Gamma$ for the Planck (*a*) and Rosseland (*b*) limit. The $\Gamma = 0$ case corresponds to conduction only.

those of the Planck radiation. They are also steeper than the Planck curves and attain smaller values of $F$ for the same values of $Z$.

Figure 2 displays the influence of the relative radiation factor $\Gamma$ upon the density $h_1$ and the temperature $\theta_1$ at the centre for both radiation limits with conduction corresponding to $\Gamma_c = 0{\cdot}001$. It reveals the same trend mentioned above; namely, that the Rosseland radiation limit reaches the isothermal bound at smaller values of $\Gamma$, numerically of the order of 1.

Results obtained for Planck radiative emission are presented in figures 3(*a*)–7(*a*) while those for Rosseland radiative diffusion are displayed in figures 3(*b*)–7(*b*). The transfer of more energy to the front, associated with larger values of $\Gamma$, is reflected in the heat-flux profiles depicted in figures 3(*a*, *b*). A more pronounced shift, of larger fluxes towards the frontal region, can be observed in the Rosseland case, figure 3(*b*), in comparison with the Planck case, figure 3(*a*).

Figures 4 and 5 give temperature and density profiles, respectively. As a result of large radiation fluxes, the temperature becomes more uniformly distributed throughout the field, with the density distribution following suit, but to a lesser extent. The effect of heat transfer on velocity is illustrated in figure 6, indicating the creation of a larger stagnant sphere around the centre as $\Gamma$ increases, extending to $x = 0{\cdot}5$ in the isothermal case. As a consequence of the fact that the increase in density does not keep pace with the temperature drop, pressure (figure 7) in the central plateau falls to a lower level than in the adiabatic case.

Although a more uniform distribution of the gasdynamic profiles is observed in these figures for Rosseland radiative diffusion in comparison with Planck radiative emission, the two limiting cases nevertheless bear a striking similarity to each other. This can be attributed to the common phenomenon in both, namely the conduction heat transfer, since, although $\Gamma_c = 0{\cdot}001$ only, the accompanying set of boundary conditions (34) at the centre impose a similar trend on both solutions near the centre. To check this conclusion, a solution for the case $\Gamma_c = 0$ was obtained for the Planck radiative-emission limit and for the general intermediate radiation case. Equations (38)

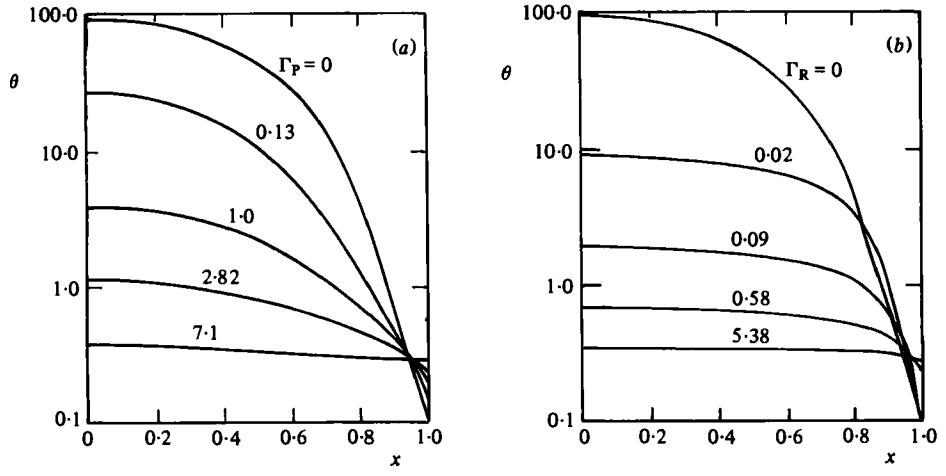


FIGURE 4. Distribution of temperature for the Planck (*a*) and the Rosseland (*b*) radiation cases.

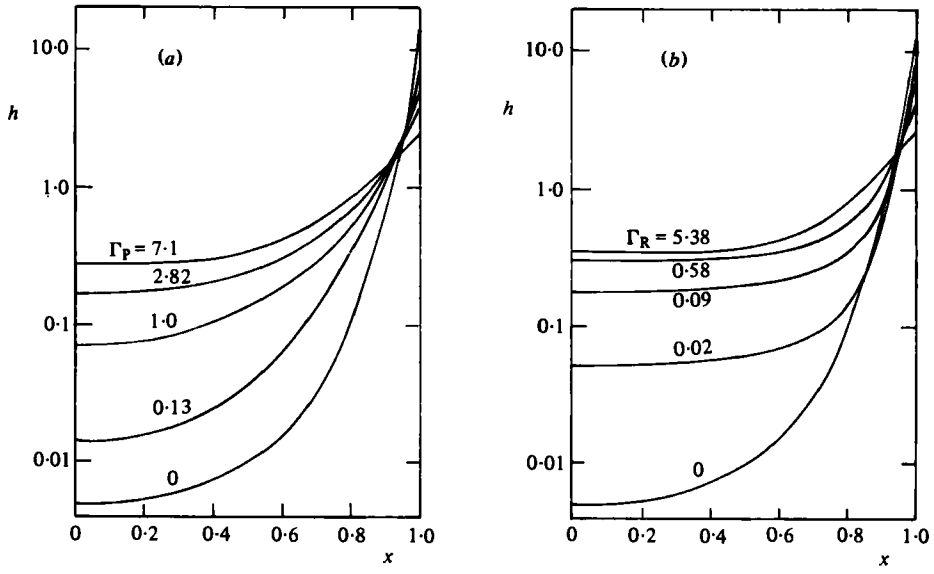


FIGURE 5. Distribution of density for different values of the radiation parameter $\Gamma$ for the Planck (*a*) and the Rosseland (*b*) radiation limits with conduction.

through (43) are used for this purpose, where for the former case $\Gamma_R$ is set equal to infinity, $I$ to zero, and (39) is used to express the variation of the radiation flux in the field, whereas for the latter case both (38) and (39) are used, with both $\Gamma_P$ and $\Gamma_R$ of the order of 1·0.

Since not all the boundary conditions at $x = 0$ are given, it is not possible to start the integration there. Thus the integration is carried out from the front using (26) to define the values of $h$, $g$, $\theta$ and $Q$ in terms of $F_n$. However, as seen from the previous cases, $F_n$ depends on the values of $\Gamma_P$ and $\Gamma_R$ and is unknown prior to the integration. This makes an iterative shooting technique necessary to find the proper value of $F_n$, to any

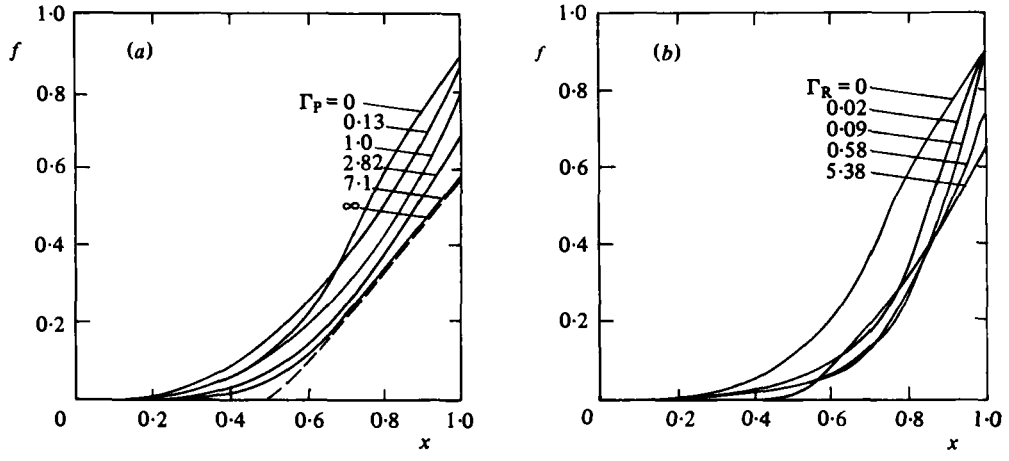


FIGURE 6. Profiles of the velocity distribution for the Planck (*a*) and the Rosseland (*b*) radiation limits. $\Gamma = 0$ corresponds to the adiabatic bound and $\Gamma = \infty$ to the isothermal bound.

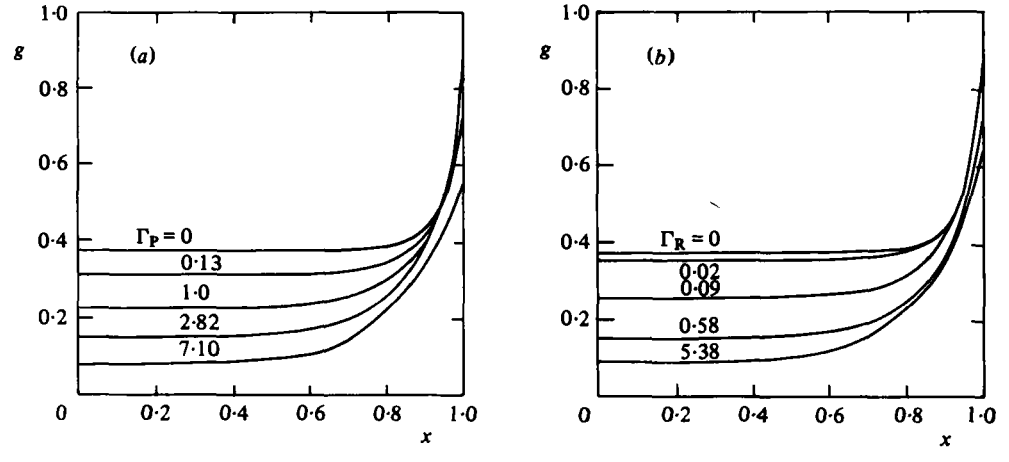


FIGURE 7. Profiles of the pressure distribution in point explosion with conduction and radiation taken into account for the Planck (*a*) and the Rosseland (*b*) limits.

desired degree of accuracy, that will lead to the satisfaction of the condition $f = 0$ at the centre. The more accurate the value of $F_n$ is, the closer one can approach the centre without encountering the saddle-point singularity there.

In the absence of conduction there is no regularity condition at the centre, and $Q = 0$ is always satisfied there, which results in a substantial deviation of this solution from the case $\Gamma_c > 0$. This situation is depicted in figures 8–13, where the Planck radiative emission case, corresponding to $\Gamma_R = \infty$, for $\Gamma_P = 0$, 1·0 and 2·0 and the intermediate case for the same values of $\Gamma_P$ and $\Gamma_R = 1{\cdot}0$ and 0·1 are compared. Figure 8 shows the phase plane for these cases. Clearly the Planck radiation curves for $\Gamma_c = 0$ strongly deviate from those of figure 1 (*a*), where $\Gamma_c = 0{\cdot}001$, especially near the front. It is interesting to notice that for decreasing $\Gamma_R$, that is, increasing absorption effects with respect to emission, the curves take on a similar trend as those for the Rosseland limit. On the one hand, the increase in $F$ near the front disappears and, on the other, the negative slopes of the curves increase at larger values of $Z$.

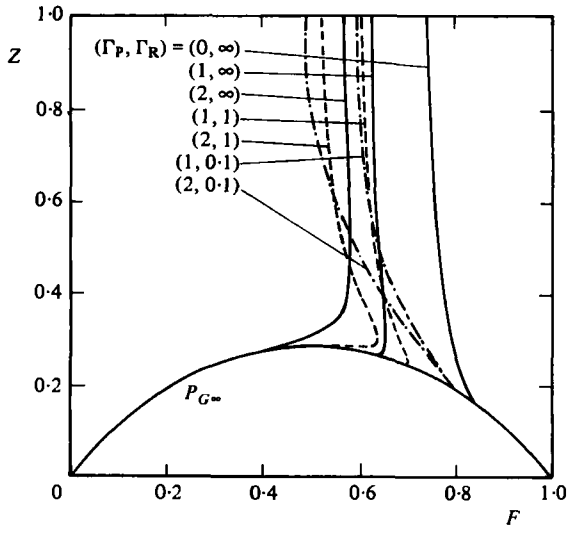


FIGURE 8. Phase plane for the $\Gamma_c = 0$ case. Planck radiative emission, corresponding to $\Gamma_R = \infty$, is shown as solid lines. The $\Gamma_R = 1{\cdot}0$ case is presented as broken lines and the $\Gamma_R = 0{\cdot}1$ case as dot–dash lines.

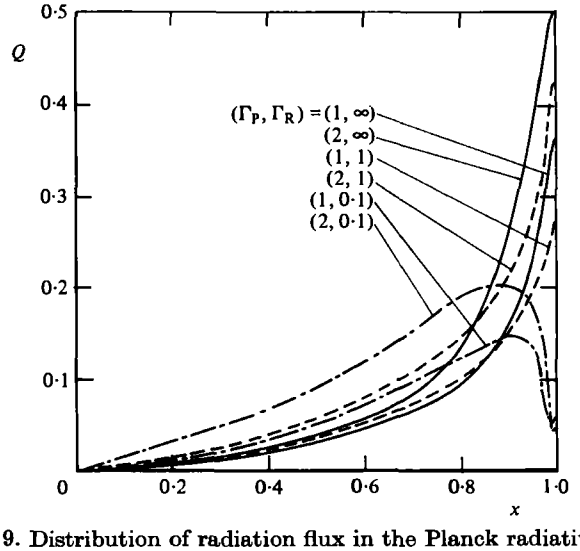


FIGURE 9. Distribution of radiation flux in the Planck radiative-emission limit and in the intermediate case, both with $\Gamma_c = 0$.

Figure 9 exhibits the variation of the radiation flux inside the field with different values of $\Gamma_P$ and $\Gamma_R$. In the Planck case, $Q_r$ is always a maximum at the front, with a sharp decrease as the centre is approached. That can be attributed to the fact that $\alpha_P$ is proportional to $h^2/\theta^{2\cdot7}$, and that $h$ decreases and $\theta$ increases sharply as the centre is approached. As the diffusion term in (23) comes into play, absorption causes the radiation flux to decrease near the front, while it increases in the interior. At smaller values of $\Gamma_R$, the profiles resemble more those of figure 4(*b*). Figures 10(*a*), (*b*) give the temperature and density distributions, respectively, where it is to be noticed that

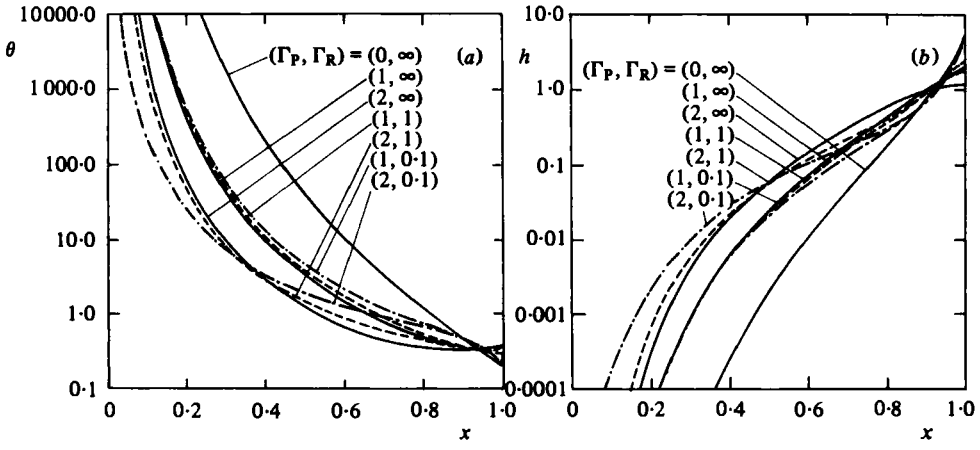


FIGURE 10. Temperature profiles (*a*) and density profiles (*b*) for Planck radiation and two intermediate radiation cases, where the radiation flux is expressed in terms of the differential approximation. Both $\Gamma_P$ and $\Gamma_R$ are $O(1)$.

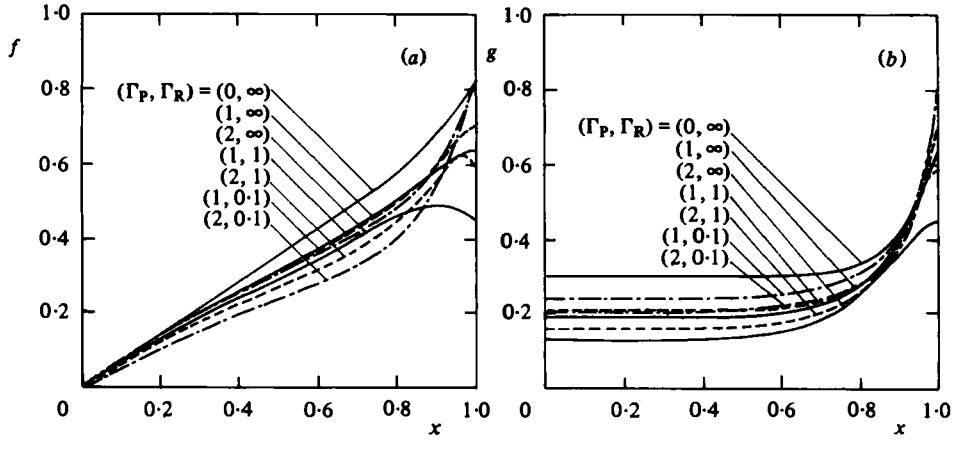


FIGURE 11. Distributions of velocity (*a*) and pressure (*b*) in point explosion with radiation, conduction neglected.

for the intermediate case $\theta$ approaches infinity and $h$ goes to zero at the centre, since the condition $Q_r = 0$ is not associated with a condition on $\theta$ or its derivative. Figure 11 (*a*) presents the corresponding velocity profiles. Strong cooling in the Planck case causes the velocity near the front to drop from its value in the interior and deviate from the more usual monotonic increase. Pressure profiles are displayed in figure 11 (*b*).

## 9. Conclusions

The problem of self-similar non-adiabatic blast waves, where both conduction and radiation are allowed to take place, was analysed. In the general case the problem can be reduced to the integration of a system of six coupled nonlinear ordinary differential equations. Our study of these equations leads to the following conclusions.

(1) Radiation, as expected, tends to produce uniform fields by attenuating the temperature gradients. However, all the energy carried by radiation is deposited on the front and the bounding shock becomes more and more overdriven. (This is demonstrated clearly in the phase planes, figures 1(*a*), 1(*b*) and 8, where the front moves along the line to the left as the radiation effects increase.)

(2) When conduction is taken into account the distribution of gasdynamic parameters in blast waves in the case of Rosseland diffusion radiation is more uniform than in the case of Planck emission radiation. With conduction neglected, the Planck emission displays, for large radiation parameters, a slight decrease in temperature near the front associated with a non-monotonic change in velocity.

(3) The case of the Rosseland thick radiation yields, in effect, the same results for self-similar blast waves as those obtained for thermal conduction (cf. Sedov 1959; Korobeinikov *et al.* 1961) because in both cases the heat flux is identical owing to the self-similarity requirements. However, the results for the Planck thin-radiation case are essentially different. This latter case does exhibit similar trends to the Rosseland limit when conduction is considered, but not when radiation is the only heat transfer mode.

(4) The general radiation case lies between the two limiting cases for intermediate values of the radiation parameters, where taking into account the diffusion–absorption term in the differential-approximation form provides the mechanism for the smooth transition from the Planck approximation to the Rosseland approximation.

This work was supported by the National Science Foundation under Grant ENG78-12372 and by the Department of Energy under Contract W-7405-ENG-48. The first author was supported by NASA Grant NAG 3-131 during the latter phases of this work.

The authors wish to thank the referees, whose insistence that results be obtained for the regime intermediate between the optically thick and thin limits led to the exposure and elucidation of important features and properties of the general radiative-transport problem.

## REFERENCES

Bowen, J. R. & Feay, B. A. 1970 A refinement of the cylindrical blast wave. *Astronautica Acta* **15**, 275–282.

Brode, H. L. 1969 Gasdynamic motion with radiation: a general numerical method. *Astronautica Acta* **14**, 433–444.

Elliot, L. A. 1960 Similarity methods in radiation and hydrodynamics. *Proc. R. Soc. Lond.* A **258**, 287–301.

Finkleman, D. & Chien, K. Y. 1968 Semigrey radiative transfer. *A.I.A.A. J.* **6**, 755–758.

Goulard, R. 1962 Similarity parameters in radiation gasdynamics. *Purdue University Rep.* A & ES 62-8.

Helliwell, J. B. 1969 Self-similar piston problem with radiative heat transfer. *J. Fluid Mech.* **37**, 497–512.

Kamel, M. M., Khater, H. A., Siefien, H. G., Rafat, N. M. & Oppenheim, A. K. 1977 A self-similar solution for blast waves with transport properties. *Astronautica Acta* **4**, 425–437.

Kim, K. B., Berger, S. A., Kamel, M. M., Korobeinikov, V. P. & Oppenheim, A. K. 1975 Boundary-layer theory for blast waves. *J. Fluid Mech.* **71**, 65–88.

Korobeinikov, V. P., Melinkova, N. S. & Ryazanov, Ye. N. 1961 *The Theory of Point Explosion*. Fizmatgiz (English transl. U.S. Dept of Commerce, JPRS 41, 334 CSO; 6961-N).

Marshak, R. E. 1958 Effect of radiation on shock wave behavior. *Phys. Fluids* **1**, 24–29.

NiCastro, J. R. 1970 Similarity analysis of radiative gasdynamics with spherical symmetry. *Phys. Fluids* **13**, 2000–2006.

Oppenheim, A. K., Lundstrom, E. A., Kuhl, A. L. & Kamel, M. M. 1971 A systematic exposition of the conservation equations for blast waves. *J. Appl. Mech.* **38**, 783–794.

Oppenheim, A. K., Kuhl, A. L., Lundstrom, E. A. & Kamel, M. M. 1972 A parametric study of self-similar blast waves. *J. Fluid Mech.* **52**, 657–682.

Sedov, L. I. 1959 *Similarity and Dimensional Methods in Mechanics*. Transl. from 4th Russian edn. Academic.

Thomas, M. & Penner, S. S. 1964 Thermal conduction and radiant energy transfer in stationary, heated air. *Int. J. Heat Mass Transfer* **7**, 1117–1122.

Traugott, S. C. 1966 Radiative heat flux potential for a nongray gas. *A.I.A.A. J.* **4**, 541–542.

Vincenti, W. G. & Kruger, C. H. 1975 *Introduction to Physical Gas Dynamics*, 2nd edn. R. E. Krieger.

Wang, K. C. 1964 The 'piston problem' with thermal radiation. *J. Fluid Mech.* **20**, 447–455.

Zel'dovich, Ya. B. & Raizer, W. P. 1967 *Physics of Shock Waves and High Temperature Hydrodynamic Phenomena*. (Transl. from 2nd Russian edn) Academic.